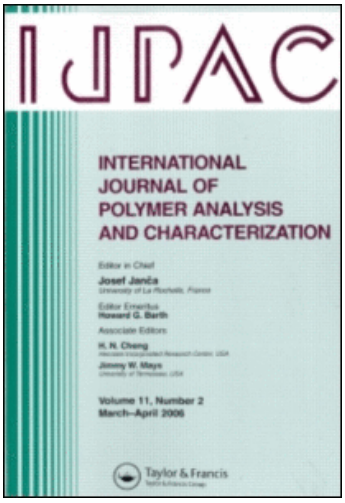

International Journal of Polymer Analysis and Characterization
Publication details, including instructions for authors and subscription information:
http://www.informaworld.com/smpp/title~content=t713646643

Combining Detectors in Size Exclusion Chromatography: II. Peak Shape Changes

R. Thitiratsakul[a]; S. T. Balke[a]; T. H. Mourey[b]
[a] Department of Chemical Engineering and Applied Chemistry, University of Toronto, Toronto, Ontario, Canada [b] Analytical Technology Division, Eastman Kodak Company, Rochester, NY

To cite this Article Thitiratsakul, R. , Balke, S. T. and Mourey, T. H.(1996) 'Combining Detectors in Size Exclusion Chromatography: II. Peak Shape Changes', International Journal of Polymer Analysis and Characterization, 2: 4, 359 — 377
To link to this Article: DOI: 10.1080/10236669608033356
URL: http://dx.doi.org/10.1080/10236669608033356

Int. J. Polymer Analysis & Characterization
1996, Vol. 2, pp. 359–377
Reprints available directly from the publisher
Photocopying permitted by license only

Combining Detectors in Size Exclusion Chromatography: II. Peak Shape Changes

R. THITIRATSAKUL and S.T. BALKE*

Department of Chemical Engineering and Applied Chemistry, University of Toronto, Toronto, Ontario M5S 3E5, Canada

and

T.H. MOUREY

Analytical Technology Division, Eastman Kodak Company, Rochester, NY 14650-2136

(Received September 28, 1995; in final form February 21, 1996)

The peak shape changes in differential viscometer (DV) chromatograms, shown in Part I of this series, were investigated. Chromatograms were obtained with narrow-molecular-weight distribution standards of increasing molecular weight. Peak shape changes were not observed when the DV detector was operated in series with the differential refractive index (DRI) detector rather than in parallel. Flowrate variations during elution of each sample in the parallel detector configuration appear to be the reason for the changes. At high molecular weights (≥460,000), polydispersity of the standards also contributed. Molecular weight averages of broad-molecular-weight distribution polymers were not affected by the detector configuration used. With a series configuration, a new method of determining interdetector volume and interpreting narrow-molecular-weight distribution polymers is presented.

KEY WORDS Size exclusion chromatography, interdetector volume, viscometer

INTRODUCTION

In Part I of this series [1], we observed that operation of a differential refractometer (DRI) and a differential viscometer (DV) in a parallel configuration yielded unexpected peak shape changes with increasing molecular weight of narrow-molecular-weight distribution standards. The normalized chromatograms were constant in shape for the DRI but became broader (and hence lower) for the DV. This observation could help to explain difficulties in obtaining interdetector volume from such chromatograms. It also could be at least partly responsible for problems in determination of the molecular weight distribution for the standards.

Presented at the 8th International Symposium on Polymer Analysis and Characterization (ISPAC-8), Sanibel Island, Florida, May 22–24, 1995.

In this work we provide additional evidence that this effect is generally present for DRI-DV detectors in parallel. Also, we examine explanations for the effect and finally, we propose how to avoid the effect and determine the molecular weight distribution of narrow standards.

THEORY

Chromatograms

Chromatograms obtained from a DRI detector include a baseline-corrected raw chromatogram (detector response versus retention volume), a concentration chromatogram (concentration versus retention volume) and a normalized chromatogram (normalized detector response versus retention volume). For the DV detector, chromatograms include the baseline-corrected raw chromatograms and the normalized chromatograms. All of these chromatograms may be plotted using retention time in place of retention volume. Appendix I reviews the various types of chromatograms and shows that the theoretical effect of flowrate and mass injected on the chromatogram depends upon the type.

The observations that motivated this work were of normalized chromatograms on a retention volume axis where the retention volume is calculated from the product of retention time and flowrate through the SEC columns. Therefore, for the DRI detector, the normalized chromatogram height, $W_N(v)$, was calculated from:

$$W_N(v) = \frac{W(v)}{\int_0^\infty W(v)\,dv} \tag{1}$$

and the normalized specific viscosity chromatogram, $\eta_{sp\,N}(v)$, from

$$\eta_{sp_N}(v) = \frac{\eta_{sp}(v)}{\int_0^\infty \eta_{sp}(v)\,dv} \tag{2}$$

As can be seen in Appendix I, *in the absence of axial dispersion effects*, the only flowrate dependence expected for these two normalized chromatograms would be the effect on the calculated retention volume. If the flowrate varies during a run and this variation is not used when calculating the product of retention time and flowrate, then the retention volume will be in error and the resulting chromatogram distorted. However, this conclusion assumes that the specific viscosity measurement by the DV is unaffected by flowrate changes.

Detector Configuration

Detectors may be arranged in a parallel (Figure 1) or series (Figure 2) configuration or, when more than two detectors are involved, some combination of the two. The parallel configuration is widely preferred because it avoids the accumulation of axial dispersion effects in chromatograms and the weakening of the DRI signal due to dilution of the

PARALLEL CONFIGURATION

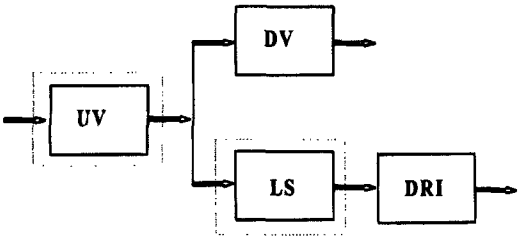

FIGURE 1 Detector arrangement in parallel configuration.

SERIES CONFIGURATION

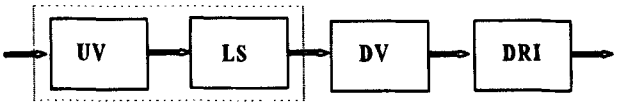

FIGURE 2 Detector arrangement in serial configuration.

stream by the DV reservoir. The DV peak shape changes published in Part I were obtained in a parallel system [1]. A weakness of the parallel system is the possibility that the flowrate in each branch may vary.

If pure solvent is used to set the flow-rate split ratio, Q_1/Q_2 at some value β then, as shown in Appendix II:

$$\frac{Q_1}{Q_2} = \beta \frac{V_1}{V_2} \frac{\int_{y-V_2}^{y} (\eta_{sp}(v)+1)\,dv}{\int_{y-V_1}^{y} (\eta_{sp}(v)+1)\,dv} \tag{3}$$

where Q_1 and Q_2 are the mobile phase flowrates through DV and DRI, β is the constant value of the ratio Q_1/Q_2 when no polymer is present (Equation II-7), V_1 and V_2 are the volumes of branches 1 and 2, y is the retention volume of interest, and $\eta_{sp}(v)$ is the specific viscosity at each retention volume.

As explained in Appendix II, this equation shows that total volume of each branch is of paramount importance in determining whether Q_1/Q_2 varies during a run. If total volumes are different in each branch, then the integration of specific viscosity over each of these volumes will yield different values and will vary as the sample elutes. As a consequence, the ratio of Q_1/Q_2 will vary during the run. Retention volume is calculated as the product of observed retention time and the mobile phase flowrate through the columns. If the Q_1/Q_2 variation affects retention volume then the shape of both DRI and DV chromatograms will be affected because the abscissa of the chromatograms are both affected.

With regards to the heights of the detector responses, the DRI should not be affected by the Q_1/Q_2 variation. However, the DV detector response is based upon measurement of pressure drop across resistances and may be influenced by flowrate variations. The DV bridge design is directed at eliminating this source of variation, and in the DV calculations, a constantly updated value of the overall pressure drop is used. However, as reported in Part I, only the DV peaks showed shape changes, and the DRI peaks were invariant.

Recently, Pigeon and Rudin [2] used two parallel detector configurations and attributed molecular weight error at the high end of the molecular weight distribution to the gradual slowing of flow through the DV and a consequent increase through the DRI. They showed that results could be improved by calculating an interdetector volume which varied with molecular weight. They did not examine the series configuration because they considered that unspecified "detector design" required both the DRI and DV to be last in any series.

With regards to detector design, the low pressure tolerance of the DRI cell is well known. However, the constraints imposed by the design of the DV are less certain. If the DRI follows the DV in series then a dilution of solution entering the DRI will result. Also, there is some concern that the diluting solvent from the DV reservoir may contain residual polymer whose concentration may vary with time.

Jackson and Barth [3] examined concerns in the practice of multiple detector size exclusion chromatography and were not deterred by such considerations. They measured peak widths of narrow-molecular-weight distribution polystyrene standards from series and parallel detector configurations. In agreement with results presented in Part I, in the parallel configuration they found the DV peaks to be slightly broader than those of the DRI. Flow-rate fluctuations or mixing occurring in the T-junctions splitting the flow in the parallel mode were suspected reasons. Also, the configuration where the DV was placed before the DRI provided the narrowest chromatograms. In this work we also examine both series and parallel configurations.

Systematic Approach

When SEC concentration and molecular weight sensitive detectors are to be used in combination, the opportunity for serious inaccuracies is greatly magnified over simple, single concentration detector systems. There are many more variables affecting results. To control this situation we have developed a method of setting up such systems, details of which have been published [4,5]. For the SEC-DV combination the method may be summarized in four steps:

Step I: Inject a broad-molecular-weight distribution polystyrene sample several times. Apply the conventional molecular weight calibration curve to the DRI chromatograms alone and calculate molecular weight averages. If these averages are of satisfactory accuracy and precision proceed to Step II.

Step II: Calculate the total intrinsic viscosity of the sample from the DV chromatograms for the sample used in Step I. If this value is of satisfactory accuracy and precision proceed to Step III.

Step III: Search for the interdetector volume, which when used with the universal calibration curve, the DV and DRI chromatograms will superimpose the calculated intrinsic viscosity calibration curve of the sample used in the above steps on the "true" intrinsic vis-

cosity calibration curve. The latter is obtained from the total intrinsic viscosities of narrow-molecular-weight distribution standards (or from a well established Mark Houwink relationship).

Step IV: Assess and, if necessary, correct for axial dispersion effects.

This approach has been found to be well suited to interpretation of SEC chromatograms from broad-molecular-weight distribution polymers, but the method does not work well for chromatograms of narrow-molecular-weight distribution polymers.

Quantitative Interpretation of Narrow-Molecular-Weight Distribution Polymers

When superimposing chromatograms obtained from narrow-molecular-weight distribution polymers, a small error in interdetector volume results in a large error in local intrinsic viscosity. The failure of methods directed at obtaining an "effective" interdetector volume, such as the "systematic approach" described above, has been ascribed to skewing in the chromatogram of a truly monodisperse sample [6]. Skewing can originate from axial dispersion effects. However, flowrate variations can also distort chromatograms (Appendix I).

A new method, which focuses directly upon peak shape, was examined. Essentially, the baseline-corrected raw DV chromatogram on a retention volume axis is matched by finding the interdetector volume and intrinsic viscosity relationship, which, when multiplied by the concentration chromatogram yields the DV chromatogram:

$$\eta_{sp}(v) = c(v - \delta)\,[\eta](v - \delta) \tag{4}$$

where $\eta_{sp}(v)$ is the specific viscosity obtained from DV and δ is the interdetector volume between the DV and the DRI detectors.

For a narrow chromatogram, it is assumed that:

$$[\eta](v - \delta) = D_1 \exp(-D_2\,(v - \delta)) \tag{5}$$

As described in Appendix III, in practice this is a two-variable search for the interdetector volume δ and the constant D_2, since the constant D_1 can be determined from the area under η_{sp}.

EXPERIMENTAL

Two different SEC systems were used in this work. System I consisted of a model 510 pump, a model 410 differential refractometer, and a model 440 UV detector with twin cells (Waters Corp., Milford, MA). The column set consisted of three PLgel 10-μm mixed-bed, 300 × 7.5-mm columns (Polymer Laboratories, Amherst, MA). The mobile phase was tetrahydrofuran (THF, BDH, Inc.) at 30°C.

System II consisted of a Spectroflow Model 757 UV detector, a Waters differential refractometer model 410, a KMX-6 LALLS photometer (Thermo Separations, Riviera Beach, FL) and a Viscotek differential viscometer model H502A (Viscotek Corp., Houston, TX). Three Polymer Lab, 5-μm mixed-bed columns were used. The mobile phase was tetrahydrofuran (THF, J.T. Baker, Inc.) at 30°C.

Narrow-molecular-weight distribution polystyrene standards from Polymer Labs were used for calibration of both systems. Concentrations of narrow-molecular-weight distribution polystyrene standards between 2.3×10^6 and 3.2×10^3 g/mol ranged from 0.5 to 6.1 mg/mL, for high-to-low molecular weights, respectively. SRM 706 broad-molecular-weight distribution polystyrene standard (National Institute of Standards and Technology, Gaithersburg, MD) was dissolved at a concentration of 1.0–1.5 mg/mL. Injection volumes were 100 μL.

RESULTS

Molecular Weight Averages

Tables I and II show the application of our systematic approach to parallel and series DV-DRI configurations. The "true" values for the molecular weight averages and intrinsic viscosity of the broad-molecular-weight distribution polystyrene standard (SRM 706) are shown in the last row of these tables. These values are recent estimates using a variety of methods and compare well with other published values [7]. The percentages are the deviations from true values. The plus and minus range given is the 95% confidence interval. These results show that good molecular weight average values can be obtained for broad-molecular-weight distribution polymers by combining DV and DRI detectors in parallel or in series configurations.

Molecular weight averages for the narrow-molecular-weight distribution standards by conventional application of the molecular weight calibration curve to the DRI chromatograms are shown in Tables III and IV. Results are generally in good agreement with those of the vendor and no significant difference between series and parallel configurations is evident.

TABLE I

Systematic approach for characterizing polystyrene SRM 706 using the parallel configuration.

	$M_n \times 10^{-3}$ (g/mol)	$M_w \times 10^{-3}$ (g/mol)	$M_z \times 10^{-3}$ (g/mol)	$[\eta]$ (dL/g)
Steps I&II	124 ± 4	282 ± 2	457 ± 15	0.95 ± 0.009
	(0.81%)	(2.17 %)	(5.06 %)	(1.06 %)
Step III	119 ± 2	277 ± 2	431 ± 8	0.94 ± 0.007
	(–3.25%)	(0.36%)	(–0.92%)	(0.0%)
true	123	276	435	0.94

TABLE II

Systematic approach for characterizing polystyrene SRM 706 using the series configuration.

	$M_n \times 10^{-3}$ (g/mol)	$M_w \times 10^{-3}$ (g/mol)	$M_z \times 10^{-3}$ (g/mol)	$[\eta]$ (dL/g)
Steps I&II	122 ± 2	282 ± 6	460 ± 12	0.95 ± 0.015
	(–0.81%)	(2.17%)	(5.75%)	(1.06%)
Step III	121 ± 6	278 ± 6	434 ± 4	0.94 ± 0.014
	(–1.63%)	(0.72%)	(–0.23%)	(0.0%)
true	123	276	435	0.94

TABLE III

Narrow-molecular-weight polystyrene standards characterized using the parallel configuration.

Standard	M_n(g/mol)		M_w(g/mol)		M_w/M_n	
M_p(g/mol)	Vendor	DRI	Vendor	DRI	Vendor	DRI
3,200	3,090	3,160	3,210	3,340	1.05	1.06
7,600	7,440	7,220	7,690	7,620	1.04	1.06
9,200	9,000	8,740	9,380[a]	9,180	1.03	1.05
34,500	33,200	32,600	34,000[a]	34,400	1.04	1.06
66,000	64,600	60,800	66,000[a]	65,800	1.03	1.08
120,000	118,000[b]	118,000	126,000[a]	124,000	1.03	1.05
156,000	152,000	144,000	162,000[a]	152,000	1.03	1.06
320,000	305,000	309,000	323,000	321,000	1.06	1.04
1,000,000	946,000	939,000	994,000[a]	1,020,000	1.05	1.09
1,290,000	1,210,000	1,200,000	1,280,000[a]	1,290,000	1.06	1.08
2,250,000	2,200,000	2,140,000	2,280,000[a]	2,220,000	1.05	1.04

note: vendor values (rounded off to three significant figures) obtained by SEC unless indicated otherwise
[a] LALLS
[b] membrane osmometry

TABLE IV

Narrow-molecular-weight polystyrene standards characterized using the series configuration.

Standard	M_n(g/mol)		M_w(g/mol)		M_w/M_n	
M_p(g/mol)	Vendor	DRI	Vendor	DRI	Vendor	DRI
3,200	3,090	3,400	3,210	3,650	1.05	1.07
7,600	7,440	7,330	7,690	7,740	1.04	1.06
9,200	9,000	8,670	9,380[a]	9,100	1.03	1.05
34,500	33,200	33,300	34,000[a]	35,000	1.04	1.05
66,000	64,600	62,200	66,000[a]	65,700	1.03	1.06
120,000	118,000[b]	114,000	126,000[a]	119,000	1.03	1.04
156,000	152,000	143,000	162,000[a]	153,000	1.03	1.07
320,000	305,000	302,000	323,000	317,000	1.06	1.05
1,000,000	946,000	951,000	994,000[a]	1,040,000	1.05	1.09
1,290,000	1,210,000	1,230,000	1,280,000[a]	1,330,000	1.06	1.08
2,250,000	2,200,000	2,130,000	2,280,000[a]	2,290,000	1.05	1.08

note: vendor values (rounded off to three significant figures) obtained by SEC unless indicated otherwise
[a] LALLS
[b] membrane osmometry

Interdetector Volume

Using System II in parallel and in series configurations with four different detectors, we calculated the interdetector volumes from the peak apices and plotted these data vs. retention volume as shown in Figures 3 and 4, respectively. From these figures it can be seen that the interdetector volume calculated in this way is generally not a function of molecular weight. The single exception is the interdetector volumes obtained for the DV detector in parallel configuration: they appear to increase with decreasing molecular weight. Interestingly, this finding is the opposite to the direction of change observed in System I. Such differences may be expected for different systems if the source of the change is the flowrate variation described by Equation (3).

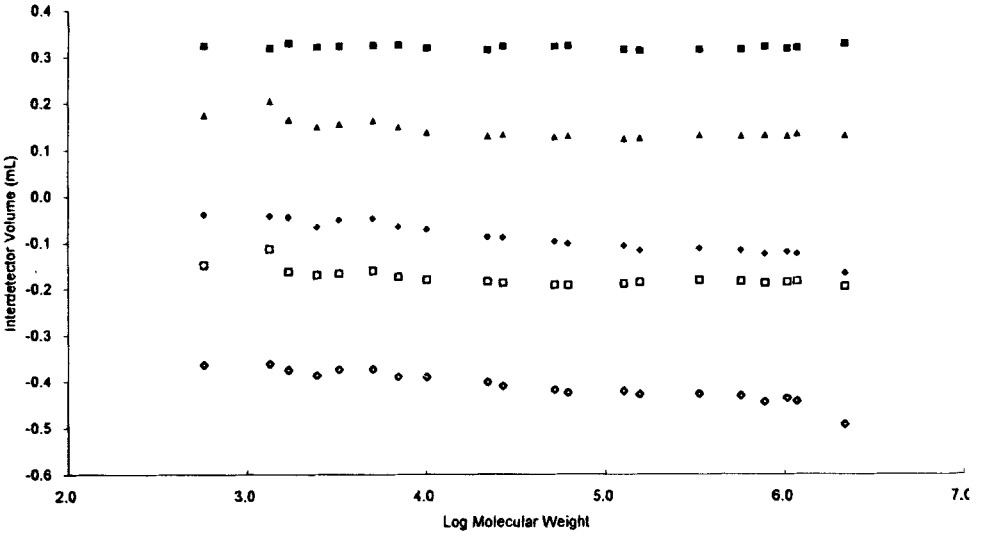

FIGURE 3 Interdetector volume versus the logarithm of the peak molecular weight of narrow-molecular-weight polystyrene fractions for detectors in parallel in System II: ■ DRI-UV; ◆ DRI-DV; ▲ DRI-LS; □ UV-LS; ◇ UV-DV.

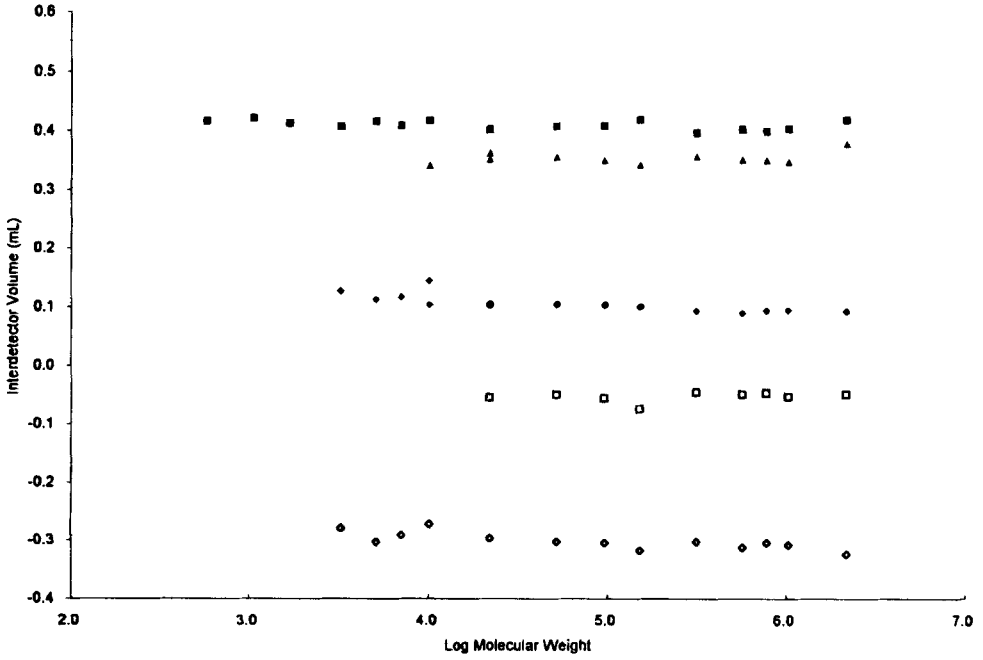

FIGURE 4 Interdetector volume versus the logarithm of the peak molecular weight of narrow-molecular-weight polystyrene fractions for detectors in series in System II. Same symbols as in Figure 3.

Peak Shape

Normalized DRI chromatograms were compared to normalized DV chromatograms for System I in parallel and series configurations. Figures 5a and 5b show the normalized DRI and DV chromatograms, respectively, for the parallel configuration (at a 40:60 split where the first value of the ratio, 40, is the percentage of the total flow passing through the DV detector and 60 is the percentage flow through the DRI branch). Each figure consists of chromatograms obtained using narrow-molecular-weight polystyrene standards ranging from 28,500 to 1,290,000 g/mol (in peak molecular weight). All chromatograms have been normalized and shifted to superimpose for comparison purposes. The DV chromatograms (Figure 5b) showed significant peak shape changes with molecular weight (the higher the molecular weight, the broader and flatter were the chromatograms) while the DRI chromatograms (Figure 5a) did not. Similar results were obtained using other parallel flow splits. However, for the detectors in a series configuration, as shown in Figures 6a and 6b no peak shape changes occurred. Thus, the cause of these changes is associated with the parallel flow operation. Flow-rate variation during a run in accord with Equation (3) was proposed as the most likely explanation; however, axial dispersion and polydispersity were other possible factors that needed to be examined. It was immediately evident that the chromatograms in Figure 6a were superimposable on those of Figure 6b. This provided some evidence that axial dispersion and polydispersity were not significant. Additional evidence was obtained by comparing three chromatograms: a normalized DRI chromatogram and a normalized DV chromatogram from DRI-DV detectors in series as well as a normalized DRI chromatogram obtained without the DV detector being present. Six sets of such chromatograms were obtained for each of three narrow molecular weight distribution standards (with peak molecular weights of 460,000, 156,000 and 28,500 g/mol) at two different flow rates (1.0 and 0.5 mL/min). Each set of three chromatograms were successfully superimposed to form a single chromatogram. In the series arrangement, as flow rate decreased, the chromatograms tended to become broader and flatter. However, both DRI and DV chromatograms were affected to the same degree. Thus, this means that if the cause of the peak shape changes in the parallel configuration is due to flow-rate variations, then the DV is sensitive to flow-rate variations during a run but not between runs.

Quantitative Interpretation of Narrow-Molecular-Weight Distribution Polymers

In matching specific viscosity chromatograms using Equation (4), two extremes are evident:

(i) If the sample is polydisperse and resolution is perfect, the true intrinsic viscosity calibration curve should apply. Equation (4) needs only to be solved for δ since the intrinsic viscosity at each retention volume is known.

(ii) If the sample is monodisperse and the spreading of the chromatogram is due almost entirely to axial dispersion, the intrinsic viscosity should be constant across the chromatogram. Again, Equation (4) needs only to be solved for δ since the intrinsic viscosity is a constant value for each standard and can be readily calculated from the DV response alone using Equation (I-13).

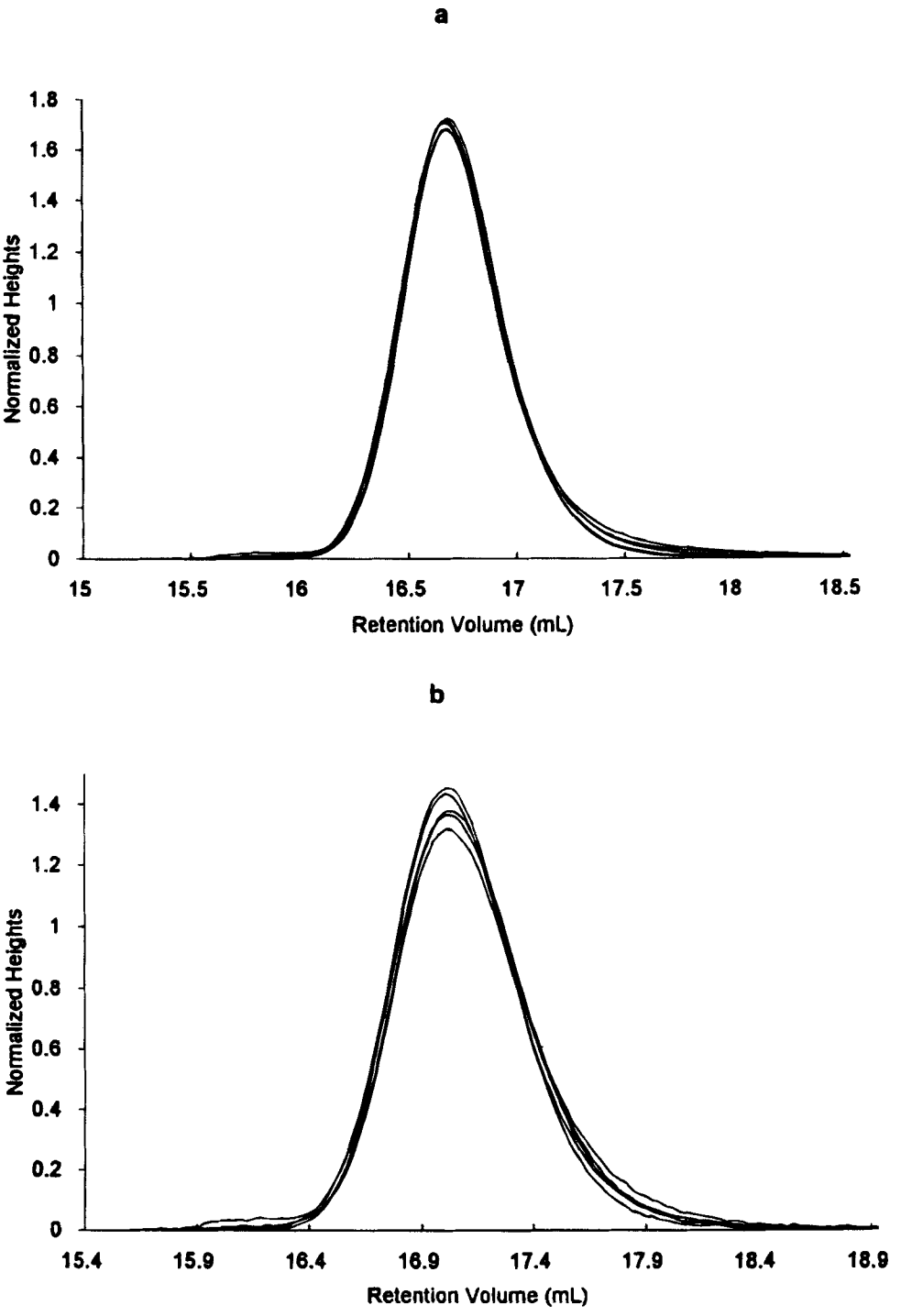

FIGURE 5 a. Normalized chromatograms from DRI detector in parallel configuration (40:60 split where the first value of the ratio is the percentage of the total flow passing through the DV detector)
b. Normalized chromatograms from DV detector in parallel configuration (40:60 split).

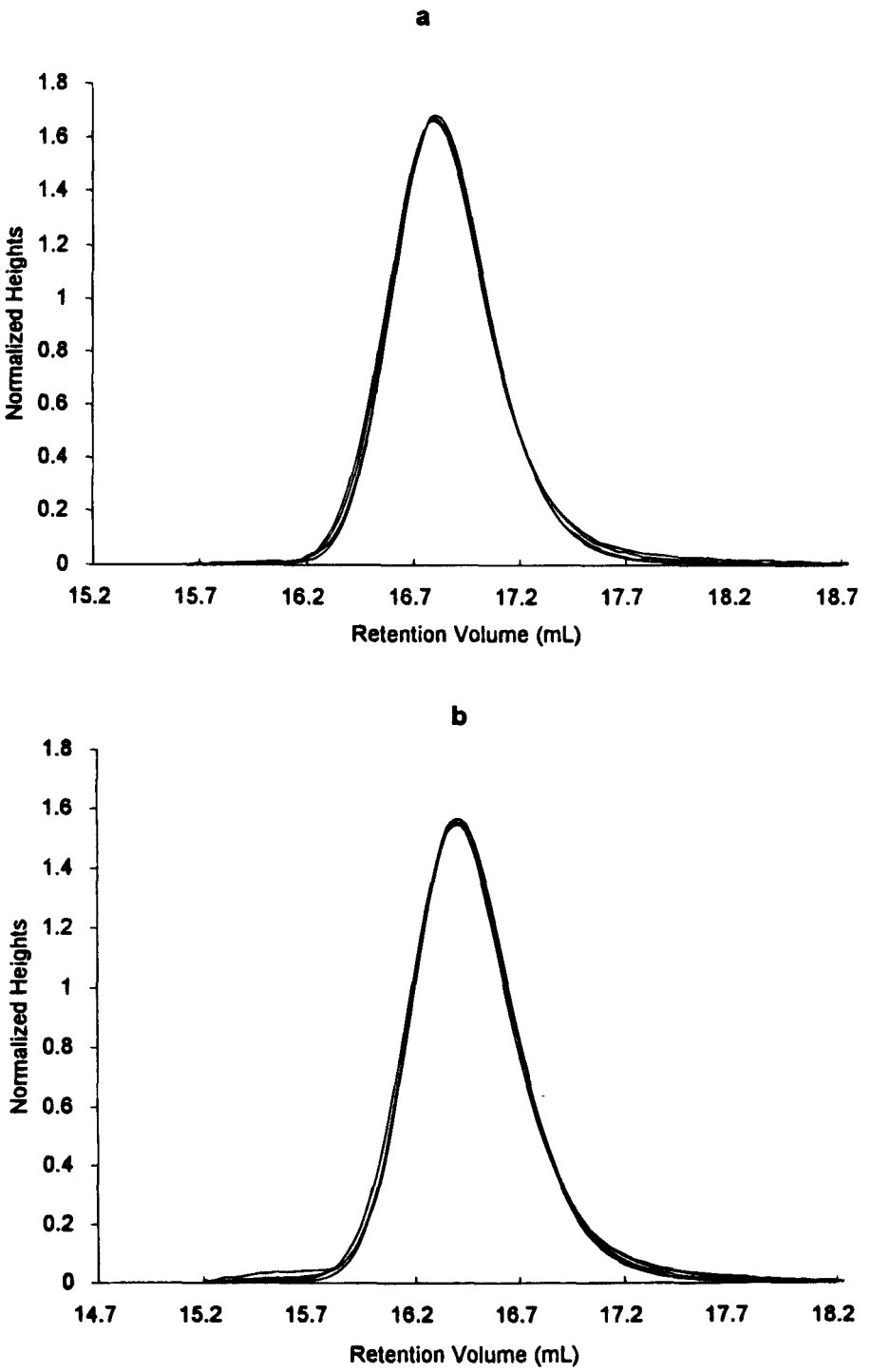

FIGURE 6 a. Normalized chromatograms from DRI detector in series configuration. b. Normalized chromatograms from DV detector in series configuration.

Whether or not either of the above extreme cases is present can be judged by examining the superposition of DV and DRI chromatograms obtained when the single parameter search for δ is performed to solve Equation (4) using the objective function of Equation (III-13).

The first step in applying this new method of interpreting narrow-molecular-weight distribution polymer begins by assuming each extreme case in turn. From this study, it was found that no good superposition of the DV and DRI chromatograms could be obtained if the first mentioned extreme case was assumed (that is, if the intrinsic viscosity calibration curve was used). The assumption of this sample being polydisperse is therefore incorrect. In the next trial of using the constant intrinsic viscosity assumption, an excellent superposition was obtained when a search for δ was conducted (for polystyrene standards of molecular weight 460,000 g/mol and less). The single parameter search for δ to match DRI and DV chromatograms actually is then identical to the "multipoint" method of determining interdetector volume published in Part I. However, in Part I only parallel flow configurations of DV and DRI detectors were examined and the determined δ values were observed to vary with molecular weight. Here we use a series detector configuration.

As shown in Table V, the interdetector volume obtained was 0.134 to 0.135 mL for the three lower molecular weight standards but differed for the 460,000 and 1,290,000 molecular weight standards. To test the hypothesis that the true interdetector volume was 0.135 mL and that the source of the superposition discrepancy was the increased polydispersity of the higher molecular weight standards, a single parameter search for D_2 was performed while maintaining δ constant at 0.135 ml. Results are shown in Table V. For the 1,290,000 molecular weight polystyrene standard, chromatogram superposition was improved and a value of D_2 of 0.088 indicated increased polydispersity in the sample was being taken into account. For the 460,000 molecular weight polystyrene standard, superposition was slightly worse and the search ended for D_2 at zero, the lower limit. Thus, polydispersity did not account for the low δ value obtained for the 460,000 molecular weight polystyrene standard. A final step in the interpretation was to conduct the full δ and D_2 search for each sample. In accomplishing this, it was again found necessary to constrain the values of D_2 to physically reasonable values (≥ 0) to avoid false minima. As Table V shows, results differed from those obtained when single parameter searches were conducted. The difficulty apparently lies with the statistical correlation between the two parameters δ and D_2. A slight increase in one can account for a slight decrease in the other while superimposing chromatograms. It is possible that improved formulation of the objective function, Equation (III-13), can overcome difficulties associated with the use of the 460,000 mole-

TABLE V

δ and D_2 search results for narrow-molecular-weight polystyrene standards.

Standard	δ Search $[\eta]$ = constant	D_2 Search $\delta = 0.135$	δ, D_2 Search $D_2 \geq 0$	
M_p (g/mol)	δ	D_2	δ	D_2
28,500	0.134	0.0	0.134	0.0
66,000	0.135	0.0	0.128	0.101
156,000	0.134	0.007	0.129	0.082
460,000	0.120	0.0	0.124	0.0
1,290,000	0.140	0.088	0.115	0.224

cular weight polystyrene standard and can obtain more accurate values of δ and D_2 when both of these parameters are searched simultaneously. However, no attempt in this direction was made at this time.

CONCLUSIONS

The DV chromatogram distortion observed for narrow-molecular-weight distribution polymers in the parallel flow configuration appeared to be significant, although variable from system to system, while distortion in peak shapes was not observed when DV and DRI detectors were used in the series configuration. Flow-rate variations are the most probable source of the distortion. However, no distortion was observed different from that exhibited by the DRI response when flowrate was varied in the series configuration between runs. It is proposed that the distortion originates from a sensitivity of the DV to flow-rate fluctuations during a run.

Interdetector volumes calculated from peak apices show a dependence on molecular weight in the parallel-flow configuration when a sufficient range of molecular weights was examined. Light scattering detectors, UV detectors, and DRI detectors in the parallel configuration, as well as all detectors in the series configuration, appear to have either no or very little such dependence.

The conventional DV equations used for calculation of specific viscosity do not appear to be the source of the chromatogram distortion. (No distortion is observed in the series configuration!)

Broad-molecular-weight distribution polymers can be analysed successfully in both series and parallel configurations.

A new method to interpret DV-DRI data from narrow-molecular-weight distribution polymers focuses attention directly upon the peak shapes and the use of the DV and DRI detectors in series. For samples which are essentially monodisperse (samples less than a peak molecular weight of 460,000 g/ml) the method is a single parameter search for the interdetector volume necessary to superimpose DV and DRI chromatograms. For narrow-molecular-weight distribution samples of significant polydispersity, the method is a search for both interdetector volume and the linear variation of the logarithm of intrinsic viscosity across the chromatogram, a two parameter search.

Acknowledgment

We wish to thank the Eastman Kodak Company (Rochester, NY) and the Natural Sciences and Engineering Research Council of Canada for funding this research. Also, we are grateful to the Canadian International Development Agency for awarding a scholarship to R. Thitiratsakul.

References

1. R. Thitiratsakul, S.T. Balke, and T.H. Mourey, *Int. J. Polym. Anal. Charact.*, **2**, 359 (1996).
2. M.G. Pigeon and A. Rudin, *J. Appl. Polym. Sci.*, **57**, 287 (1995).
3. C. Jackson and H.G. Barth, In *Chromatographic Characterization of Polymer: Hyphenated and Multidimensional Techniques*; T. Provder, H.G. Barth and M.W. Urban, Eds.; Advances in Chemistry 247; American Chemical Society: Washington, DC, 1995; pp 60–68.

4. T.H. Mourey and S.T. Balke, In *Chromatography of Polymers*; T. Provder, Ed.; ACS Symposium Series 521; American Chemical Society: Washington, DC, 1993; pp 180–198.
5. S.T. Balke, R. Thitiratsakul, R. Lew, P. Cheung, and T.H. Mourey, In *Chromatography of Polymers*; T. Provder, Ed.; ACS Symposium Series 521; American Chemical Society: Washington, DC, 1993; pp 199–219.
6. P. Cheung, R. Lew, S.T. Balke, and T.H. Mourey, *J. Appl. Polym. Sci.*, **47**, 1701 (1993).
7. T.H. Mourey, S.M. Miller and S.T. Balke, *J. Liq. Chromatogr.*, **13**, 435(1990).

APPENDIX I: CHROMATOGRAMS IN SIZE EXCLUSION CHROMATOGRAPHY CHROMATOGRAMS FROM THE CONCENTRATION DETECTOR

The most fundamental chromatogram obtained from a concentration detector is the baseline-corrected raw chromatogram. The output from a differential refractometer (as an example of that from a concentration detector), is a plot of the signal in mv ($W(t)$) vs. each measured corresponding retention time t. The total mass of polymer injected m is then proportional to the area under the chromatogram:

$$m = K \int_0^\infty W(t)\, dt \tag{I-1}$$

where the proportionality constant K is given by:

$$K = \frac{dc}{dn}\frac{dn}{dV} Q \tag{I-2}$$

where c = concentration [mg/mL], n = refractive index of the solution [RI units], V = voltage [mv], and Q = flow rate [mL/min]. Note that the units of the quantity under the integral sign are mv min. The constant K converts these units to mg.

To work in retention volume v rather than time t to avoid flow-rate effects, $W(v)$ is plotted vs. v in which $W(v)$ is the mv signal at each value of Qt and is numerically equal to the value of $W(t)$. The relationship between mass m and the area under $W(v)$ vs. v, the retention volume-based raw chromatogram, is given by:

$$m = K_1 \int_0^\infty W(v)\, dv \tag{I-3}$$

where the new constant K_1 is given by:

$$K_1 = \frac{dc}{dn}\frac{dn}{dV} \tag{I-4}$$

If we define $W(\log M)\, d(\log M)$ as the weight of polymer with log M from log M to log $M + d(\log M)$, then, this must be equal to the weight of polymer from retention volume v to $v + dv$ and the weight of polymer from retention time t to $t + dt$. That is:

$$W(\log M)\, d(\log M) = -K\, W(t)\, dt = -K_1\, W(v)\, dv \tag{I-5}$$

$W(\log M)$ is the weight of polymer in the log M increment per log M increment. $W(\log M)$ is a "weight density" analogous to "population density" in statistics and the distribution is a

differential distribution. In contrast, $W(t)$ and $W(v)$ are simply voltage readings (not voltage per increment of time or retention volume). If we divide through by m, using Equations (I-1) and (I-3), then the normalized concentration chromatogram height $W_N(v)$, is

$$W_N(v) = \frac{W(v)}{\int_0^\infty W(v)\,dv} \tag{I-6}$$

and the various ordinates are related by:

$$W_N(\log M)\,d(\log M) = -W_N(t)\,dt = -W_N(v)\,dv \tag{I-7}$$

Equation (I-7) states that the weight fraction (and hence the area) under each corresponding increment on the abscissa of each plot ($W_N(\log M)$ vs. $\log M$, $W_N(t)$ vs. t and $W_N(v)$ vs. v) are equal. $W_N(\log M)$, $W_N(t)$, and $W_N(v)$ can all be defined as "weight fraction densities" since they each represent weight fraction divided by some increment (in $\log M$, time or retention volume, respectively). $W_N(\log M)$ vs. $\log M$ is a normalized, differential molecular weight distribution, $W_N(t)$ vs. t is a normalized time-based chromatogram, and $W_N(v)$ vs. v is a normalized retention volume-based chromatogram. The total area under any one of these normalized chromatograms is unity and the corresponding area fractions obey Equation (I-7).

Concentration at each retention time $c(t)$ can be calculated from:

$$c(t) = \frac{m}{dv} W_N(t)\,dt \tag{I-8}$$

$$c(t) = \frac{m}{Q\,dt} W_N(t)\,dt = \frac{m}{Q} W_N(t) \tag{I-9}$$

or $c(t)$ plotted vs. t is a time-based raw concentration chromatogram. From Equation (I-8) we can see that the area under $c(t)$ vs. t is m/Q.

The concentration at any retention volume, v, $c(v)$ can be calculated from:

$$c(v) = \frac{m}{dv} W_N(v)\,dv = m\,W_N(v) \tag{I-10}$$

$c(v)$ plotted vs. v is a retention volume-based raw concentration chromatogram. From Equation (I-10) it is evident that the area under $c(v)$ vs. v is the total mass injected.

CHROMATOGRAMS FROM THE DIFFERENTIAL VISCOMETER DETECTOR

The DV detector provides the specific viscosity at each retention time $\eta_{sp}(t)$. A plot of these values provides a time-based specific viscosity chromatogram. As in the case of a concentration chromatogram, retention time would depend upon mobile phase flow rate. Normally, the abscissa is changed to retention volume and the values of η_{sp} are plotted vs. Qt to provide a plot of $\eta_{sp}(v)$ vs. v (a retention volume-based specific viscosity chromatogram). This chromatogram would be expected to be unaffected by small changes in flowrate. In addition, the latter chromatogram is preferred over the former because the cal-

culation of the total intrinsic viscosity obtained from the area under the specific viscosity chromatogram is based upon the total intrinsic viscosity of a sample being the weighted sum of the component intrinsic viscosities:

$$[\eta] = \sum_{0}^{\infty} w_i [\eta]_i \tag{I-11}$$

where $[\eta]$ is the total intrinsic viscosity of the sample and $[\eta]_i$ is the intrinsic viscosity of weight fraction w_i of the sample. This can be written as:

$$[\eta] = \sum_{0}^{\infty} \frac{c_i}{\sum_{0}^{\infty} c_i} \frac{\eta_{sp_i}}{c_i} \tag{I-12}$$

Now, cancelling the c_i and dividing numerator and denominator by dv, we obtain the usual equation:

$$[\eta] = \frac{\int_0^{\infty} \eta_{sp}(v)\,dv}{\int_0^{\infty} c(v)\,dv} = \frac{\int_0^{\infty} \eta_{sp}(v)\,dv}{m} \tag{I-13}$$

If we divide by dt instead of dv in order to use $c(t)$ vs. t and $\eta_{sp}(t)$ instead of $c(v)$ vs. v and $\eta_{sp}(v)$, then the denominator of Equation (I-13) will be m/Q (a much less preferable situation because of the flow-rate dependence).

Normalized specific viscosity chromatograms can be obtained on both a time and a retention volume basis. From Equation (I-13) we see that the area under a plot of $\eta_{sp}(v)$ vs. v is equal to the product of the mass injected and the total intrinsic viscosity. Thus, we define a normalized specific viscosity ordinate on a retention volume basis, $\eta_{sp\,N}(v)$ as:

$$\eta_{sp_N}(v) = \frac{\eta_{sp}(v)}{\int_0^{\infty} \eta_{sp}(v)\,dv} = \frac{\eta_{sp}(v)}{m[\eta]} = \frac{[\eta](v)}{[\eta]} \frac{c(v)}{m} \tag{I-14}$$

The plot of $\eta_{sp\,N}(v)$ vs. v has an area of unity and would be expected to be unaffected by flowrate (assuming negligible axial dispersion effects). In contrast, if the normalized chromatogram is defined in terms of $\eta_{sp}(t)$, then the denominator of Equation (I-14) would be $m[\eta]/Q$ and therefore the area would increase as the flowrate increased.

APPENDIX II: FLOW-RATE VARIATION IN THE PARALLEL DETECTOR CONFIGURATION

For multiple detectors in a parallel configuration, the total pressure drop in DV branch must be equal to that in the DRI branch,

$$\Delta P_1 = \Delta P_2 \tag{II-1}$$

where ΔP_1 is the pressure drop in the DV branch and ΔP_2 is the pressure drop in the DRI branch.

From the Hagen Poiseuille equation for laminar Newtonian flow in a tube, the pressure drop in the DV and DRI branches in Equation (II-1) can be expressed in terms of mobile phase flowrate and viscosity:

$$\frac{8Q_1\eta_1 V_1}{\pi^2 r_1^6} = \frac{8Q_2\eta_2 V_2}{\pi^2 r_2^6} \tag{II-2}$$

where Q_1 and Q_2 are the mobile phase flowrates through DV and DRI, η_1 and η_2 are the viscosities of the liquid flowing through DV and DRI, V_1 and V_2 are the volume of the tubing in the DV and DRI branches, and r_1 and r_2 are the radii of the tubing in each branch.

Consider the pressure drop across each branch to consist of the sum of pressure drops across a series of small incremental volumes, each dv in length. If the steady state is assumed and the viscosity is constant only across one of these small increments, then the expression in Equation (II-2) can be written in terms of volume of the bridge and with η as a continuous function of volume:

$$\frac{8Q_1}{\pi^2 r_1^6}\int_{y-V_1}^{y}\eta_1(v)\,dv = \frac{8Q_2}{\pi^2 r_2^6}\int_{y-V_2}^{y}\eta_2(v)\,dv \tag{II-3}$$

Rearranging to obtain a ratio of Q_1/Q_2:

$$\frac{Q_1}{Q_2} = \frac{r_1^6}{r_2^6}\frac{\int_{y-V_2}^{y}\eta_2(v)\,dv}{\int_{y-V_1}^{y}\eta_1(v)\,dv} \tag{II-4}$$

or

$$\frac{Q_1}{Q_2} = \frac{r_1^6}{r_2^6}\frac{\int_{y-V_2}^{y}(\eta_{sp2}(v)+1)\,dv_2}{\int_{y-V_1}^{y}(\eta_{sp1}(v)+1)\,dv_1} \tag{II-5}$$

If pure solvent is used to set the flow split at a ratio β, then

$$\eta_{sp2}(v) = \eta_{sp1}(v) = 0 \tag{II-6}$$

and

$$\frac{Q_1}{Q_2} = \frac{r_1^6 V_2}{r_2^6 V_1} = \beta \tag{II-7}$$

Solving function r_1^6/r_2^6 and substituting in Equation (II-7) gives:

$$\frac{Q_1}{Q_2} = \beta\frac{V_1}{V_2}\frac{\int_{y-V_2}^{y}(\eta_{sp2}(v)+1)\,dv_2}{\int_{y-V_1}^{y}(\eta_{sp1}(v)+1)\,dv_1} \tag{II-8}$$

If the volume of each branch is equal then, according to Equation (II-8), the flow rate should remain constant during a run. For example, if a 50:50 flowrate split is obtained by adding more tubing to one branch, then equal volumes and a constant flow rate during operation may thus result. However, as can be seen from Equation (II-7), it is possible to obtain equal volumes for each branch ($V_1 = V_2$) in this way for $\beta = 1$ only if the radius of tubing (and cells) in each branch can be considered equal ($r_1 = r_2$). If the volume in one branch is different from the other, then the integration in Equation (II-8) will be over different limits for each branch and viscosity will contribute more to one branch than the other. This will cause a variation in flow split during a run and a distortion in the chromatogram.

APPENDIX III: QUANTITATIVE INTERPRETATION OF NARROW-MOLECULAR-WEIGHT DISTRIBUTION SAMPLES

From the definition of a local intrinsic viscosity:

$$[\eta](v) = \frac{\eta_{sp}(v)}{c(v)} \tag{III-1}$$

When a DV detector is used to obtain $\eta_{sp}(v)$ and a concentration detector is used to obtain $c(v)$ then the interdetector volume between the two detectors must be taken into account:

$$[\eta](v - \delta) = \frac{\eta_{sp}(v)}{c(v - \delta)} \tag{III-2}$$

Thus, specific viscosity can be expressed as:

$$\eta_{sp}(v) = c(v - \delta)\,[\eta](v - \delta) \tag{III-3}$$

We are given $\eta_{sp}(v)$ and $c(v - \delta)$ but δ and $[\eta](v - \delta)$ are unknown. Multiply by dv and integrate:

$$\int_0^\infty \eta_{sp}(v)\,dv = \int_0^\infty c(v - \delta)[\eta](v - \delta)\,dv \tag{III-4}$$

The left-hand side of the equation is readily obtainable as the area under the DV chromatogram (A_{DV}).

$$\int_0^\infty \eta_{sp}(v)\,dv = A_{DV} \tag{III-5}$$

Thus,

$$A_{DV} = \int_0^\infty c(v - \delta)[\eta](v - \delta)\,dv \tag{III-6}$$

For a narrow-molecular-weight distribution, a good assumption is that the intrinsic viscosity at $v - \delta$ obeys:

$$[\eta](v - \delta) = D_1 \exp(-D_2(v - \delta)) \tag{III-7}$$

$$[\eta](v - \delta) = D_1 \exp(-D_2 v) \exp(D_2 \delta) \tag{III-8}$$

$$[\eta](v - \delta) = D_1^* \exp(-D_2 v) \tag{III-9}$$

where

$$D_1^* = D_1 \exp(D_2 \delta) \tag{III-10}$$

Thus,

$$A_{DV} = \int_0^{\alpha} c(v - \delta)_i \, D^*_1 \exp(-D_2 v) \, dv \tag{III-11}$$

$$D^*_1 = \frac{A_{DV}}{\int_0^{\alpha} c(v - \delta)_i \exp(-D_2 v) \, dv} \tag{III-12}$$

Therefore, a two-parameter numerical search for δ and D_2 can be implemented to solve Equation (III-3) and provide both δ and $[\eta](v - \delta)$ by minimizing:

$$O(\delta, D_2) = \sum_{i=1}^{n} w_i (\eta_{sp}(v_i) - c(v_i - \delta)[\eta](v_i - \delta))^2 \tag{III-13}$$

where the weighting factor w_i is $1/\eta_{sp}(v_i)^2$ if it is assumed that the percentage error in $\eta_{sp}(v_i)$ is a constant.